Large Optical Nonlinearity of Semiconducting Single-Walled Carbon Nanotubes under Resonant Excitations

A. Maeda,[1] S. Matsumoto,[1] H. Kishida,[1,2] T. Takenobu,[3,4] Y. Iwasa,[3,4] M. Shiraishi,[5] M. Ata,[6] and H. Okamoto[1,*]

[1]*Department of Advanced Materials Science, University of Tokyo, Chiba 277-8561, Japan*
[2]*PRESTO, Japan Science and Technology Agency, Chiba 277-8561, Japan*
[3]*Institute for Materials Research, Tohoku University, Sendai 980-8577, Japan*
[4]*CREST, Japan Science and Technology Agency, Kawaguchi 332-0012, Japan*
[5]*Graduate School of Engineering Science, Osaka University, Osaka 560-8531, Japan*
[6]*National Institute of Science and Technology (AIST), Ibaraki 305-8565, Japan*

(Received 25 March 2004; published 3 February 2005)

We measured third-order nonlinear susceptibility ($\chi^{(3)}$) spectra in semiconducting single-walled carbon nanotubes (SWNTs) by the *Z*-scan method. $|\mathrm{Im}\chi^{(3)}|$ is remarkably enhanced under resonant excitation to the lowest interband transition, reaching 4.2×10^{-6} esu and 1.5×10^{-7} esu in SWNTs grown by the laser ablation and HiPco methods, respectively. A comparison of the transient absorption changes evaluated by degenerate and nondegenerate pump-probe measurements suggests that the resonant enhancement of $|\mathrm{Im}\chi^{(3)}|$ is dominated by a coherent process rather than by saturation of absorption.

DOI: 10.1103/PhysRevLett.94.047404 PACS numbers: 78.67.Ch, 42.65.–k, 78.47.+p

The rapid progress of the optical communication network demands all optical switching devices which enable terahertz control of phase, amplitude, and route of lights. For the realization of such ultrafast control of lights, nonlinear optical (NLO) materials with large third-order nonlinear susceptibility $\chi^{(3)}$ and small relaxation time of photocarriers are indispensable. One-dimensional (1D) materials are good candidates of NLO materials, since quantum confinement of electron-hole motion on 1D space can enhance $\chi^{(3)}$. Recently, the high potential of single-walled carbon nanotubes (SWNTs) as NLO materials has been suggested from both the experimental and the theoretical point of view [1–8]. Semiconducting SWNTs (SC-SWNTs) have the lowest absorption peak around the optical fiber communication wavelength (1.55 μm). Its optical nonlinearity is therefore attracting interest concerning possible applications to optical switching devices as well as academic interest in the field of physics and chemistry.

Quantitative evaluation of $\chi^{(3)}(-\omega; \omega, -\omega, \omega)$ around the absorption peak of SC-SWNTs has been reported by two groups on SWNTs synthesized by the high pressure decomposition of carbon monoxide (the HiPco method). One was given by a pump-probe (PP) measurement with a 150 fs laser pulse [5], in which $\mathrm{Im}\chi^{(3)}$ near the absorption peak (1.55 μm) was roughly estimated as -10^{-10} esu. Another was given by using a *Z*-scan method with a 200 fs laser pulse [6]. The study showed that $\mathrm{Im}\chi^{(3)}$ at the absorption peak (1.3 μm) is fairly large, reaching -8.5×10^{-8} esu. In both studies as well as in other NLO studies on SWNTs, observed third-order optical nonlinearity around the gap transition has been attributed to saturation of absorption. There has, however, been no spectroscopic study of $\chi^{(3)}$, and therefore the mechanism for the enhancement of $\chi^{(3)}$ has not been fully understood yet. The time characteristic of the optical response has also been investigated by several groups using PP methods [5,6,9–11]. Those studies revealed that the relaxation time of photoexcited states in SC-SWNTs is very fast, being less than 1 ps. The origin for such an ultrafast optical response has, however, not been clarified yet.

In this Letter, we report quantitative $\mathrm{Im}\chi^{(3)}(-\omega; \omega, -\omega, \omega)$ spectra of the two kinds of SWNTs synthesized by the laser ablation and the HiPco method, which are abbreviated in the following as L-SWNT and H-SWNT, respectively. By using the *Z*-scan method [12], $\mathrm{Im}\chi^{(3)}$ was evaluated in the whole energy region of the gap transition in the SC-SWNTs. $|\mathrm{Im}\chi^{(3)}|$ was found to be remarkably enhanced under resonant excitation to the gap transition, reaching 4.2×10^{-6} esu in L-SWNTs and 1.5×10^{-7} esu in H-SWNTs. We also studied time characteristics of the optical response in the two SWNTs by PP measurements under the resonant excitation condition and evaluated the relaxation time T_1. The results revealed that the figure of merit (FOM) for third-order optical nonlinearity in SWNTs is very large as compared with that of conventional semiconductors. In addition, by comparing the responses for the resonant excitation and off-resonant one, we demonstrate that the enhancement of optical nonlinearity under the resonant excitation condition is dominated mainly by a coherent process rather than by an incoherent one, such as saturation of absorption.

L-SWNTs were made by the method previously reported [13]. From the energy dispersive x-ray spectroscopy, the catalyst impurities (Ni) were found to be very small, being just 1 at.%. H-SWNTs were purchased from Carbon Nanotechnologies, Inc. and used without further purification. Thin film samples were prepared by spraying SWNTs suspended in ethanol under sonication on CaF_2 substrates. The absorption spectrum of the L- (H-)SWNT film with the

 © 2005 The American Physical Society

thickness L_s of ~160 nm (130 nm) is presented in Fig. 1. The absorption band at 0.6–1.1 eV corresponds to the lowest interband transition of SC-SWNTs, on which we focus in this study. The broadening of this band is due to distributions of tube diameter d. It is known that the average d value of H-SWNTs (~0.9 nm) is smaller than that of L-SWNTs (~1.4 nm), and the interband transition energy is approximately proportional to d^{-1} [14]. As a result, in H-SWNTs, the peak energy of the absorption band is relatively large.

In both the Z-scan and PP measurements, we used laser pulses with 110 fs duration obtained from optical parametric amplifiers pumped by a Ti:Al_2O_3 regenerative amplifier system operating at 1 kHz. To evaluate $\mathrm{Im}\chi^{(3)}$ of the films by the Z-scan method, we used a SiO_2 plate as a reference, in which the absolute value of the nonlinear refractive index n_2 is known. The linear refractive index n_0 and the extinction coefficient κ_0, which are also necessary to evaluate $\mathrm{Im}\chi^{(3)}$, were obtained by analyzing the results of ellipsometry, absorption, and reflectance measurements. The detailed procedure to determine $\mathrm{Im}\chi^{(3)}$ using SiO_2 as a reference has been reported in Ref. [15]. In the PP measurement, we detect time evolution of the transmittance change $\Delta T(t)/T$ and deduce the photoinduced change $\Delta\alpha(t)$ of absorption coefficient α from $\Delta T(t)/T$ using the following relations:

$$\Delta\alpha(t) = \Delta\alpha_0(t) \times \exp(-\alpha_{\mathrm{pump}} x), \tag{1}$$

$$\Delta\alpha_0(t) = -\frac{\alpha_{\mathrm{pump}} \ln[\Delta T(t)/T + 1]}{1 - \exp(-\alpha_{\mathrm{pump}} L_s)}. \tag{2}$$

Here, α_{pump} is the linear absorption coefficient for the pump light in the sample, $\Delta\alpha_0(t)$ is the absorption change of the probe light at the sample surface, and x is the distance from the sample surface.

A typical Z-scan profile from the L-SWNT film in the open-aperture condition [12] is presented in Fig. 2(a). Magnitudes of the signals are characterized by $f^{-1}(T(0))$, which is proportional to the photoinduced change of α at the sample surface for $z = 0$. Here, $f(x) = [\ln(x+1)]/x$. For an accurate evaluation of $\mathrm{Im}\chi^{(3)}$ by the Z-scan method, we have to adjust the intensity of the incident light P_s so that $f^{-1}(T(0))$ is proportional to P_s. In Fig. 2(b), we show the P_s dependence of $-f^{-1}(T(0))$ at around the absorption peak (0.704 eV in L-SWNTs and 0.970 eV in H-SWNTs). $-f^{-1}(T(0))$ is proportional to P_s for $P_s < 0.3$ nJ (1.0 nJ) and is saturated for $P_s \sim 4$ nJ (30 nJ) in L- (H-)SWNTs. All the $\mathrm{Im}\chi^{(3)}$ measurements shown below are performed in the condition that $-f^{-1}(T(0))$ is proportional to P_s. In the PP measurements, we also adjusted the pump power, I_{pump}, as $\Delta\alpha_0(0)$ is proportional to I_{pump}.

The $-\mathrm{Im}\chi^{(3)}$ spectra of L-SWNTs and H-SWNTs obtained by the Z-scan method are presented in Fig. 3, together with n_0 and κ_0. Maximum values of $|\mathrm{Im}\chi^{(3)}|$ ($\max|\mathrm{Im}\chi^{(3)}|$) are very large, reaching 4.2×10^{-6} esu in L-SWNTs and 1.5×10^{-7} esu in H-SWNTs. To compare the spectral shape of $\mathrm{Im}\chi^{(3)}$ with that of the linear absorption for the interband transition, we subtracted the background from the ϵ_2 spectrum around the band gap region. The obtained ϵ_2 spectra are shown in Fig. 3 by the gray lines, the spectral shapes of which are quite similar to those of $\mathrm{Im}\chi^{(3)}$. This similarity indicates that the observed NLO

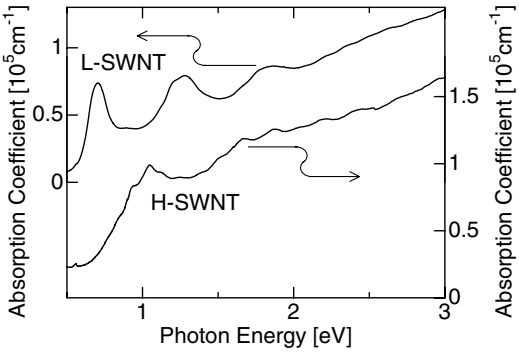

FIG. 1. Absorption spectra of L-SWNTs and H-SWNTs.

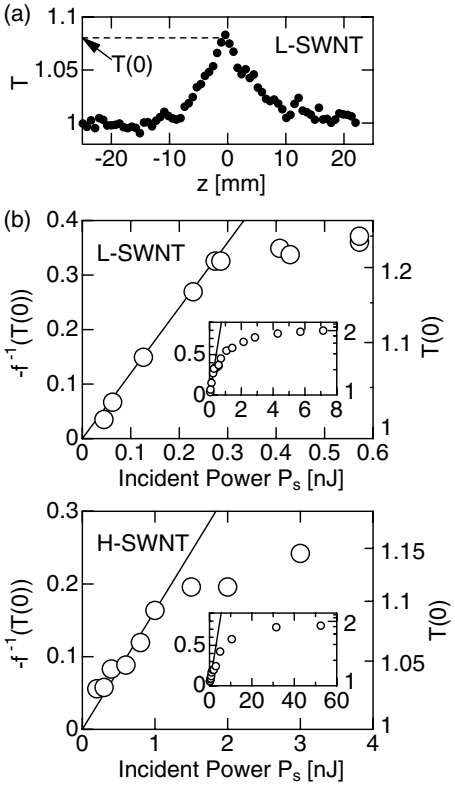

FIG. 2. (a) Typical Z-scan profile of the L-SWNT film in the open-aperture configuration at 0.704 eV. (b) Incident-power dependences of $-f^{-1}(T(0))$ in L-SWNTs at 0.704 eV and in H-SWNTs at 0.970 eV. The solid lines show a linear relation between $-f^{-1}(T(0))$ and the incident power.

response is due to the photoinduced change of the absorption spectrum associated with SC-SWNTs.

Another important result about the optical nonlinearity is the time characteristics of the response. In Figs. 4(a) and 4(b), we present the time evolutions of $-\Delta\alpha_0$ obtained by the PP measurement with degenerate configuration, in which both the pump energy (E_{pump}) and the probe energy (E_{probe}) are set at the absorption peak indicated by the solid arrow in Fig. 3 (0.688 eV for L-SWNTs and 0.953 eV for H-SWNTs). The observed time characteristics cannot be explained by a single exponential decay but are composed of the two components: the ultrafast component and the slower one, the decay times of which are much shorter and longer than the pulse duration of 110 fs, respectively. We simulated $-\Delta\alpha_0$ with the following equation including the convolution of the pump and probe pulses:

$$-\Delta\alpha_0(t) = A_1 \exp\left[-\left(\frac{t}{\tau}\right)^2\right] + A_2 \exp\left(-\frac{t}{T_1}\right) \times \frac{\int_{-\infty}^{t} \exp[t'/T_1 - (t'/\tau)^2]dt'}{\int_{-\infty}^{0} \exp[t'/T_1 - (t'/\tau)^2]dt'}. \quad (3)$$

Here, τ is the parameter associated with the pulse duration. A_1 and A_2 are the amounts of the ultrafast and slow components at $t = 0$, respectively. $-\Delta\alpha_0(t)$ is well reproduced by Eq. (3), as shown by the solid lines in Figs. 4(a) and 4(b). τ is set to 110 fs, and the other parameters are $A_1 = 1.24 \times 10^4$ (1.57×10^3), $A_2 = 4.37 \times 10^3$ (5.06×10^2), and $T_1 = 0.90$ ps (0.35 ps) for L- (H-)SWNTs. The calculated ultrafast and slow components are represented by the shaded area and the broken line, respectively. $A_1/(A_1 + A_2)$ is about 0.75 in both SWNTs, indicating that the ultrafast response dominates the large optical nonlinearity.

The experimental configuration of the degenerate PP measurement at $t = 0$ ps is the same as that of the Z-scan method, so we can compare the $\text{Im}\chi^{(3)}$ values deduced in the two methods. $\text{Im}\chi^{(3)}$ can be calculated from the magnitudes of $\Delta\alpha_0(0)$ using the formula $\text{Im}\chi^{(3)} = \epsilon_0 c^2 n_0^2/(3\omega I_{\text{pump}})\Delta\alpha_0(0)$. Here, ϵ_0 is the permittivity of vacuum and c the light velocity. The obtained $-\text{Im}\chi^{(3)}$ is 3.0×10^{-6} esu (1.8×10^{-7} esu) for L- (H-)SWNTs, which is fairly consistent with that evaluated from the Z-scan method.

To clarify the origin of the two components in the time characteristics, we performed nondegenerate (two-color) PP measurements, in which only E_{pump} is shifted to the higher energy at 0.739 eV (1.022 eV) for L- (H-)SWNTs, which is indicated by the open arrow in Fig. 3. The time evolutions of $-\Delta\alpha_0(t)$ are shown in Figs. 4(c) and 4(d), which can be reproduced by the single exponential component as shown by the solid line. The obtained parameters are $A_2 = 1.53 \times 10^3$ (1.22×10^2) and $T_1 = 1.0$ ps (0.35 ps) for L- (H-)SWNTs. The values of T_1 are almost equal to those evaluated from the degenerate PP measurements. Since the similar slower component is observed in the degenerate and two-color PP measurements in common, it is attributable to saturation of absorption, that is, incoherent NLO response. Namely, T_1 reflects the decay

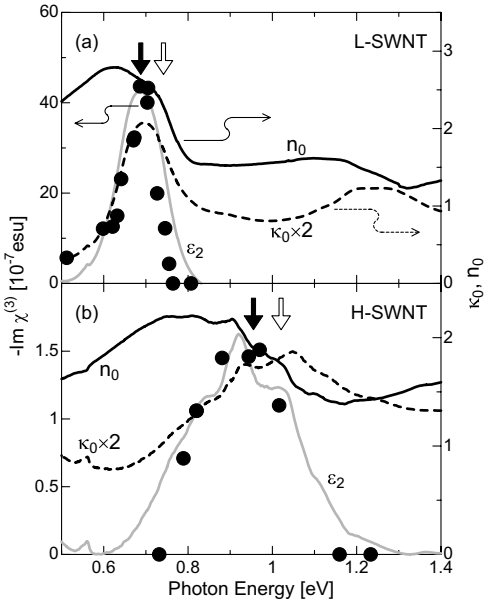

FIG. 3. $-\text{Im}\chi^{(3)}$ spectra (solid circles) of L-SWNTs (a) and H-SWNTs (b). n_0 and κ_0 are also shown by the solid and dashed lines, respectively. The gray lines show the normalized ϵ_2 spectra, in which the background [the straight line from 0.50 eV (0.60 eV) to 0.83 eV (1.31 eV) for L- (H-)SWNTs] is excluded. The solid and open arrows indicate the energy positions of the pump light used in the degenerate and nondegenerate PP measurements shown in Fig. 4, respectively.

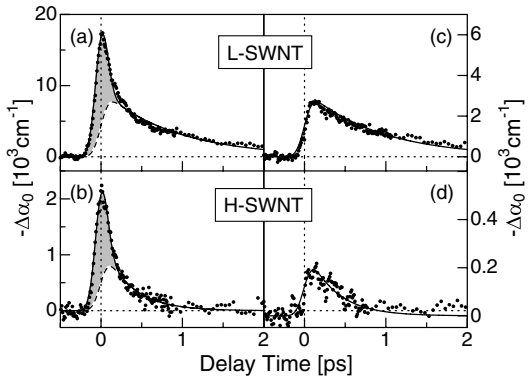

FIG. 4. Time characteristics of $-\Delta\alpha_0$ (solid circles) in L- and H-SWNTs with the degenerate [(a),(b)] and the nondegenerate [(c),(d)] condition [(a) $E_{\text{pump}} = E_{\text{probe}} = 0.688$ eV; (b) $E_{\text{pump}} = E_{\text{probe}} = 0.953$ eV; (c) $E_{\text{pump}} = 0.739$ eV, $E_{\text{probe}} = 0.688$ eV; and (d) $E_{\text{pump}} = 1.022$ eV, $E_{\text{probe}} = 0.953$ eV]. Solid lines show the fitting curves by Eq. (3). The shaded area and the broken line in (a) and (b) show the ultrafast and slow components, respectively.

time of the photoexcited states. Very recently, it has been reported that the relaxation process of the photoexcited states in the micelle-suspended isolated SC-SWNTs occurs with the decay time of ~10 ps [16], which is much longer than that reported previously in the SWNT films [5,6,9–11] and that evaluated in our SWNT films. It has been ascertained from the transmission electron microscope measurement that our SWNT films are composed of the bundles. It is, therefore, reasonable to consider that the relaxations with T_1 of 1 ps (0.35 ps) for L-SWNTs (H-SWNTs) will be dominated by charge transfer and/or energy transfer of the photoexcited electrons and holes to neighboring metallic tubes, as suggested previously [10].

On the other hand, the ultrafast component is observed only for the degenerate PP measurement. Therefore, it is reasonably attributed to the coherent NLO response. This coherent response is interpreted as an optical Stark effect and a stimulated emission. As for the NLO response of SC-SWNTs, Margulis *et al.* theoretically suggested the importance of the coherent response characteristic of the two-level system [2,3]. The ultrafast response observed in our study is essentially the same with what they proposed. They also discussed the contribution of the combined process of the intrerband-intraband transitions to the NLO response, which gives the two-photon absorption (TPA). In our study, however, $\mathrm{Im}\chi^{(3)}$ is always negative and the increase of the absorption is not observed. To examine the TPA process, more detailed studies such as the PP spectroscopy should be necessary.

The degenerate PP experiments under resonant excitation have been previously reported on the bundled SWNTs [6,10] and on the isolated SWNTs [16]. In these studies, the increase of the transmittance was attributed to saturation of absorption. In the former studies, the pulse width of the used laser is not so small, being 200 fs [6] and 180 fs [10]. Considering the convolution of pump and probe pulses, the time resolution will be larger than 250 fs. In the latter study [16], the time resolution also seems not to be so high, probably because the sample is in a liquid state. Such low time resolutions might be the reason why the coherent process was not clearly seen in those studies.

As detailed above, the NLO response at $t = 0$ ps in the degenerate PP measurement is dominated mainly by the ultrafast response, that is, the coherent process. In fact, $\max|\Delta\alpha_0|$ at $t \approx 0$ ps in the two-color PP measurement is about one-sixth (one-eleventh) of that observed in the degenerate PP one for L- (H-)SWNTs. From these results, large $-\mathrm{Im}\chi^{(3)}$ obtained by the Z-scan method is also attributable mainly to the coherent process.

In addition to $\mathrm{Im}\chi^{(3)}$, we measured $\mathrm{Re}\chi^{(3)}$ in L-SWNTs at 0.756 eV (1.64 μm) using the closed-aperture condition [12] of the Z-scan method (not shown). The obtained $\mathrm{Re}\chi^{(3)}$ reaches $(1.3 \pm 0.2) \times 10^{-6}$ esu, which is as large as $-\mathrm{Im}\chi^{(3)}$. It demonstrates that the optical control of the refractive index will also be possible in SWNTs.

When we consider the applications of NLO materials, it is more practical to evaluate FOM defined as $|\mathrm{Im}\chi^{(3)}|/(\alpha T_1)$. In this sense, the bundled SWNTs with $T_1 \sim 1$ ps will be more advantageous than the isolated SWNTs with $T_1 \sim 10$ ps. By using the values of $|\mathrm{Im}\chi^{(3)}|$, α, and T_1 evaluated in this study, FOM is deduced to be 68 esu cm/s at 1.8 μm in L-SWNTs and 6.3 esu cm/s at 1.4 μm in H-SWNTs. The value in L-SWNTs is tremendously larger than those of other semiconductors: 0.010 esu cm/s at 0.90 μm in GaAs [17,18] and 2.6 esu cm/s at 0.94 μm in polydiacetylene [19–22], which is well known to show large optical nonlinearity. In SWNTs, the optical gap is tunable by the control of tube diameter and large FOM will be obtained at 1.55 μm. Judging from these facts, it can be concluded that SWNTs are strong candidates for future NLO materials.

In summary, we have measured $\mathrm{Im}\chi^{(3)}$ spectra by the Z-scan method in SWNTs. The $\max|\mathrm{Im}\chi^{(3)}|$ is fairly large, reaching 4.2×10^{-6} esu and 1.5×10^{-7} esu in L-SWNTs and H-SWNTs, respectively. A comparison of degenerate and nondegenerate pump-probe measurements suggests that the enhancement of $|\mathrm{Im}\chi^{(3)}|$ under resonant excitation is due to a coherent process rather than an incoherent one, such as saturation of absorption. In addition, the value of the figure of merit for SWNTs is much larger than that for other semiconductors, demonstrating the high potential of SWNTs as NLO materials.

*Corresponding author.
Electronic address: okamotoh@k.u-tokyo.ac.jp

[1] R.-H. Xie and J. Jiang, J. Appl. Phys. **83**, 3001 (1998).
[2] V. A. Margulis, J. Phys. Condens. Matter **11**, 3065 (1999).
[3] V. A. Margulis and E. A. Gaiduk, J. Opt. A Pure Appl. Opt. **3**, 267 (2001).
[4] X. Liu *et al.*, Appl. Phys. Lett. **74**, 164 (1999).
[5] Y.-C. Chen *et al.*, Appl. Phys. Lett. **81**, 975 (2002).
[6] S. Tatsuura *et al.*, Adv. Mater. **15**, 534 (2003).
[7] Y. Sakakibara *et al.*, Jpn. J. Appl. Phys. **42**, L494 (2003).
[8] S. Yamashita *et al.*, Opt. Lett. **29**, 1581 (2004).
[9] M. Ichida *et al.*, Physica (Amsterdam) **323B**, 237 (2002).
[10] J.-S. Lauret *et al.*, Phys. Rev. Lett. **90**, 057404 (2003).
[11] O. J. Korovyanko *et al.*, Phys. Rev. Lett. **92**, 017403 (2004).
[12] M. Sheik-Bahae *et al.*, IEEE J. Quantum Electron. **26**, 760 (1990).
[13] H. Kataura *et al.*, Appl. Phys. A **74**, 1 (2002).
[14] H. Kataura *et al.*, Synth. Met. **103**, 2555 (1999).
[15] A. Maeda *et al.*, Phys. Rev. B **70**, 125117 (2004).
[16] G. N. Ostojic *et al.*, Phys. Rev. Lett. **92**, 117402 (2004).
[17] H. S. Loka *et al.*, IEEE J. Quantum Electron. **34**, 1426 (1998).
[18] T. Skauli *et al.*, J. Appl. Phys. **94**, 6447 (2003).
[19] G. M. Carter *et al.*, Appl. Phys. Lett. **49**, 998 (1986).
[20] T. Fehn *et al.*, Appl. Phys. B **59**, 203 (1994).
[21] B. Lawrence *et al.*, Phys. Rev. Lett. **73**, 597 (1994).
[22] A. Feldner *et al.*, Opt. Commun. **195**, 205 (2001).